# Fluorescent Carbon Nanoparticles: Synthesis, Characterization, and Bioimaging Application

**ARTICLE** *in* THE JOURNAL OF PHYSICAL CHEMISTRY C · OCTOBER 2009

Impact Factor: 4.77 · DOI: 10.1021/jp905912n



**4 AUTHORS**, INCLUDING:

Sekhar C Ray
University of South Africa
**97** PUBLICATIONS **1,535** CITATIONS
SEE PROFILE

Arindam Saha
Indian Association for the Cultivation of Sci…
**28** PUBLICATIONS **724** CITATIONS
SEE PROFILE

Nikhil R Jana
Indian Association for the Cultivation of Sci…
**113** PUBLICATIONS **9,741** CITATIONS
SEE PROFILE

# Fluorescent Carbon Nanoparticles: Synthesis, Characterization, and Bioimaging Application

**S. C. Ray,[†,*] Arindam Saha, Nikhil R. Jana,* and Rupa Sarkar**

*Centre for Advanced Materials, Indian Association for the Cultivation of Science, Kolkata-700032 India*

*Received: June 24, 2009; Revised Manuscript Received: September 20, 2009*

Fluorescent carbon nanoparticles (CNPs) 2−6 nm in size with a quantum yield of about ∼3% were synthesized via nitric acid oxidation of carbon soot, and this approach can be used for milligram-scale synthesis of these water-soluble particles. These CNPs are nanocrystalline with a predominantly graphitic structure and show green fluorescence under UV exposure. Nitric acid oxidation induces nitrogen and oxygen incorporation into soot particles, which afforded water solubility and a light-emitting property; the isolation of small particles from a mixture of different sized particles improved the fluorescence quantum yield. These CNPs show encouraging cell-imaging applications. They enter into cells without any further functionalization, and the fluorescence property of these particles can be used for fluorescence-based cell imaging applications.



## Introduction

The emergence of fluorescence carbon nanoparticles (CNPs) shows high potential in biological labeling, bioimaging, and other different optoelectronic device applications.[1−13] These carbon nanoparticles are biocompatible and chemically inert,[2,6,14−18] which has advantages over conventional cadmium-based quantum dots.[19] However, these fluorescent carbon nanoparticles are poorly studied compared with other carbon-based materials, such as carbon nanotubes and fullerenes. In addition, the understanding of the origin of fluorescence in carbon nanoparticle is far from sufficient.[4,5,7,9] For example, information on the microstructure and surface ligands remains unclear and details of the organic passivation is not sufficient to aid understanding of the surface states beneficial for light emission.

Common routes in making fluorescent carbon nanoparticles include high-energy ion beam radiation based creation of point defects in diamond particles, followed by annealing;[1,3] laser ablation of graphite, followed by oxidation and functionalization;[4,7] thermal decomposition of organic compounds;[10,11,13] electrooxidation of graphite;[9] and oxidation of candle soot with nitric acid.[8] A wide range of fluorescent carbon particles of different colors can be prepared by those approaches; for example, octadecylamine-functionalized diamond nanoparticle showed blue fluorescence,[12] nitrogen-doped diamonds showed red fluorescence,[1a] and candle soot derived particles,[8] thermal decomposition method,[11,13] or laser ablation method[4] produced particles with multiple colors. However, the quantum yield of most of these particles is too low (<1%),[8,9] with few exceptions.[4,13] In addition, the synthetic methods are cumbersome and inefficient. For example, in the high-energy ion beam radiation based method, it is difficult to introduce a large number of point defects into ultrafine nanocarbon particles (<10 nm) for bright luminescence.[1,3] Thermal decomposition based methods produce a low yield of soluble and fluorescent particles with a significant fraction of insoluble product.[10,11,13] Soot-based synthesis produces a particle mixture of different colors, and isolation of different colored particles by gel electrophoresis is a difficult task.[8] A recent report showed that surface passivation can lead to a significant increase in fluorescence quantum yield (4−15%); however, the exact mechanism is not yet clear.[4,13] Thus, simple, efficient, and large-scale synthesis of fluorescent carbon nanoparticles and their isolation, purification, and functionalization are very challenging.

Among all these synthetic methods, the soot-based approach is simple and straightforward.[8] However, the quantum yield of fluorescent carbon nanoparticles is too low (<0.1%) for any useful application.[8] Herein, we report an improved soot-based method of synthesizing fluorescent carbon nanoparticles (CNPs) 2−6 nm in size with a quantum yield of ∼3%. There are three distinct improvements in our modified method. First, we developed a simple separation method of small size and fluorescent carbon particles from the heterogeneous particle mixture. The method is applicable for milligram-scale synthesis of these particles. Second, small particles are more fluorescent than larger ones and thus isolation of small particles improves the quantum yield from <0.1% to ∼3%. Third, we observed that these small carbon particles enter into cells without any further functionalization and the fluorescence property of the particles can be used for fluorescence-based cell-imaging applications.

## Experimental Procedures

**Synthesis of Carbon Particles.** Carbon soot (25 mg, collected from a burning candle) was mixed with 15 mL of 5 M nitric acid in a 25 mL three-necked flask. It was then refluxed at 100 °C for 12 h with magnetic stirring. After that, the black solution was cooled and centrifuged at 3000 rpm for 10 min to separate out unreacted carbon soot. The light brownish-yellow supernatant was collected, which shows green fluorescence under UV exposure. The aqueous supernatant was mixed with acetone (water/acetone volume ratio was 1:3) and centrifuged at 14 000 rpm for 10 min. The black precipitate was collected and dissolved in 5−10 mL of water. The colorless and nonfluorescent supernatant was discarded. This step of purification separates excess nitric acid from the carbon nanoparticles. This concentrated aqueous solution, having almost neutral pH, was taken for further use. The same synthesis technique was also performed for 6 h of reflux and 18 h of reflux. The supernatant obtained from the 6 h reflux was pale yellow and, for the 18 h reflux, was dark yellow. We weighed the unreacted carbon soot, which was removed as precipitate, in order to find

* To whom correspondence should be addressed. E-mail: raysekhar@rediffmail.com) (S.C.R.), camnrj@iacs.res.in (N.R.J.).
[†] Present address: School of Physics, University of the Witwatersrand, Private Bag 3, Wits 2050, South Africa.

10.1021/jp905912n CCC: $40.75 
Published on Web 10/07/2009

out the yield of soluble carbon nanoparticles. The weight was ~22.5 mg for the 6 h reflux time (yield ~10%) and ~20 mg for the 12 and 18 h reflux times (yield ~20%). It shows that yield increases as reflux time increases from 6 to 12 h but, after that, no significant increases was observed. This solution has particles having sizes ranging from 20 to 350 nm and are called as-synthesized carbon particles (CPs) (see Scheme 1).

**SCHEME 1: Steps in the Preparation of Fluorescent Carbon Nanoparticles (CNPs) from Soot**

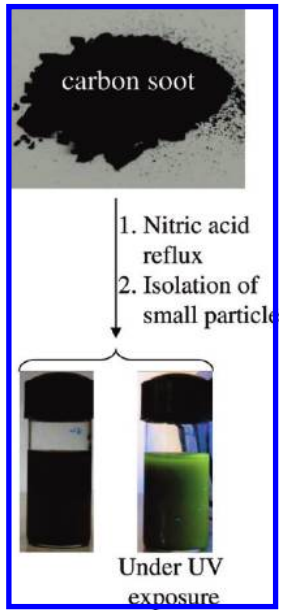


**Size Separation of Carbon Particles.** Size separation was performed in a solvent mixture with the combination of high-speed centrifuge based separation. As-synthesized carbon particles (CPs) are soluble in water, ethanol, and acetone but insoluble in chloroform. The aqueous and ethanolic particle solutions do not precipitate even at 16 000 rpm centrifugation. So we chose a solvent mixture of water−ethanol−chloroform (single phase without any phase separation) for the size separation of particles where water−ethanol helps to solubilize the particles but chloroform decreases their solubility. Next, we followed a step-by-step separation using different centrifugation speeds from 4000 to 16 000 rpm.

In a typical process, the aqueous solution of carbon nanoparticles was mixed with chloroform and ethanol, maintaining a water/chloroform/ethanol volume ratio of 1:1:3. Next, 2 mL of this solution was centrifuged with 4000 rpm for 10 min. The precipitate was collected and dissolved in 2 mL of fresh water. The supernatant was then again centrifuged at 5000 rpm for 10 min, and the precipitate was collected and redissolved in 2 mL of water. The same procedure was applied at 6000 and 8000 rpm. The supernatant obtained after 8000 rpm was not getting precipitated even at 16 000 rpm. This solution was collected and evaporated to dryness to remove ethanol and chloroform and finally dissolved in water. This solution has particle sizes of 2−6 nm and are named as carbon nanoparticles (CNPs) that were used for characterization and application. The yield of CNPs from CPs is ~50%, which means 25 mg of soot can produce ~2−3 mg of CNPs. In this calculation, we assumed that carbon dioxide formation is negligible during nitric acid oxidation.

**Cell Labeling and Cytotoxicity Assay.** For the cell labeling experiment, Ehrlich ascites carcinoma cells (EAC) were collected from the peritoneal cavity of adult female mice after 7 days of inoculation. The suspension of cells was prepared with a concentration of ~$10^7$ cell/mL. Next, 1.0 mL of this suspension was mixed with 10−100 $\mu$L of aqueous CNP solution and incubated for 30 min. Next, labeled cells were separated from free CNPs by centrifuging at 2000 rpm for 3 min. The precipitated cells were suspended in phosphate buffer solution. This type of precipitation-resuspended was repeated two more times, and finally, cells were suspended in phosphate buffer solution. A drop of this suspension was placed in a glass slide for imaging experiment. The fluorescence image was captured using an Olympus IX71 fluorescence microscope with a DP70 digital camera.

For MTT and Trypan blue assays, HepG2 cells were trypsinized and resuspended in culture medium. The cells were seeded to a flat bottom microplate with 0.5 mL full of medium and kept for overnight at 37 °C and 5% $CO_2$. The CNP solution of different amounts was loaded to each well, and each concentration has three duplications. After incubation for 24 h, 50 $\mu$L of MTT solution (5 mg/mL) was added to each well 4 h before the end of the incubation. The medium was discarded, and produced formazan was dissolved with DMSO. The plates were read with an absorbance at 550 nm. The optical density is directly correlated with cell quantity, and cell viability was calculated by assuming 100% viability in the control set without any CNP. In the case of the Trypan blue assay, 0.4% of Trypan blue solution was used instead of MTT and, after 5 min, stained cells are counted to determine the cell viability.

**Instrumentation.** Diluted CNP solution was dropped onto copper grids to prepare specimens for transmission electron microscopic (TEM) observation, which was performed in a FEI Tecnai G2 F20 microscope with a field emission gun operating at 200 kV. The microstructures of the CNPs were examined using a JEOL JSM-6700F scanning electron microscope and a Veeco di CP-II atomic force microscope. The fluorescence (photoluminescence) spectra were measured on a Hitachi F4500 fluorescence spectrophotometer at different excitation energies, ranging from 325 to 600 nm. A Nicolet 6700 Fourier transform infrared (FTIR) spectrophotometer was used to analyze chemical bonds on the surface of CNPs. A PerkinElmer PH1−1600 X-ray photoelectron spectrometer (XPS) was used for compositional analysis and chemical bond determination of CNPs. The dynamic light scattering (DLS) study was performed using a model BI-200SM instrument (Brookhaven Instrument Corporation), after filtering the sample solution with a Milipore syringe filter (0.2 $\mu$m pore size). Micro Raman studies were performed using an ISA Lab Raman system equipped with a 514.5 nm laser with a 100× objective, giving a spot size about 1 $\mu$m with a spectral resolution better than 2 $cm^{-1}$. The quantum yield was measured by comparing the integrated photoluminescence intensities and absorbance values of the CNPs with the reference fluorescein dye (QY = 95%).

## Results and Discussion

Carbon soot is black in color and completely insoluble in water even after ultrasonnication. This is because they are large in size and hydrophobic in nature. When this soot is refluxed with nitric acid, light brown colored supernatant solution is obtained along with an insoluble black precipitate. A brownish-yellow supernatant indicates a part of the carbon particles becomes small and water-soluble during the refluxing processes. This soluble particle exhibits green fluorescence when irradiated with UV light, while the precipitate part shows no fluorescence. We have studied the fluorescence spectra at different excitation

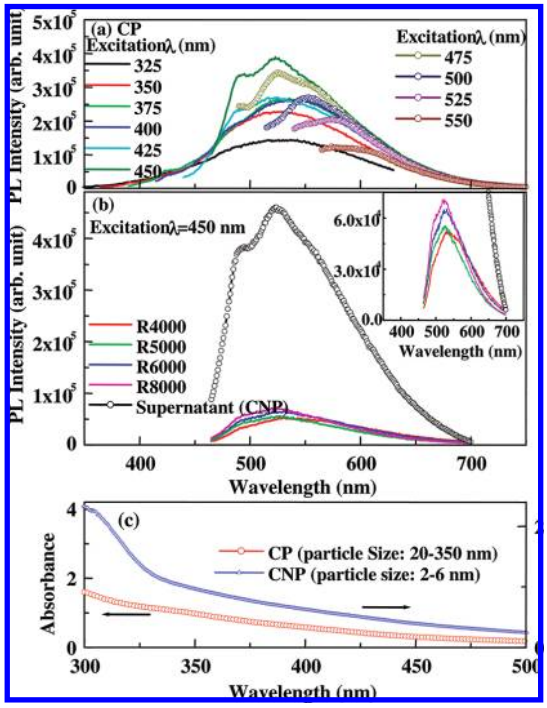


**Figure 1.** (a) Fluorescence spectra of as-synthesized aqueous carbon particles (CPs), obtained by 12 h refluxing, excited at different wavelengths. (b) Fluorescence spectra of different sized CPs, showing the most intense spectrum for the smallest size (shown as supernatant, which corresponds to a CNP of 2−6 nm). The as-synthesized CP solution was dissolved in 2 mL of water−ethanol−chloroform solution and then centrifuged at different speeds. After each step of centrifugation, the precipitate was dissolved in 2 mL of fresh water. The smallest sized CP (shown as supernatant) does not precipitate even at 16 000 rpm. All the solutions are excited at 450 nm. (c) UV−visible absorption spectra of an aqueous solution of as-synthesized carbon particles (CPs) and smallest sized carbon particles of 2−6 nm (CNPs).

energies, ranging from 325 to 600 nm and found that the highest fluorescence intensity was achieved at the excitation wavelength of 450 nm, which shows an emission maximum at 520 nm. Figure 1a shows the photoluminescence spectra of as-synthesized CPs with different excitation wavelengths. We have tested the quality and yield of CPs as a function of reflux time and found that 12 h is the optimum time. If the reflux time is less, the yield is low, and for longer reflux time, the yield does not increase appreciably. (see the Experimental Procedures and Figure S1a in the Supporting Information).

The nature of the fluorescence spectra suggested that there are different types of particles with different colors. Earlier work also showed that these particles can be separated by gel electrophoresis technique.[8] We have performed size separation of CPs in order to separate CPs of different fluorescent property. The size separation has been performed in a solvent mixture with the combination of high-speed centrifuge based separation. We have identified the mixture of water−ethanol-chloroform as a single phase solvent for the effective size separation of CPs, where water−ethanol helps to solubilize the CPs but chloroform decreases their solubility. Next, we have followed a step-by-step separation using different centrifugation speeds from 4000 to 16 000 rpm. Figure 1b shows the fluorescence spectra of CP solution after successive size separation. It shows that the smallest particle (CNP) that does not precipitate, even at 16 000 rpm, shows the highest fluorescence. All the other size particles show very weak fluorescence, and there is very little blue shift in the fluorescence with decreasing particle size. The fluorescence study of various phosphate buffer solutions of CNPs shows that fluorescent intensity does not change appreciably on solution pH from 7 to 9. (see Figure S1b, Supporting Information). The comparative absorption spectra of as-synthesized carbon particles (CPs) and the smallest particles (CNPs) are shown in Figure 1c. No appreciable change is observed, except that CNPs show a stronger absorbance in the visible wavelength along with a weak band at ∼350 nm.

The transmission electron microscopic (TEM) study shows that as-synthesized carbon particles (CPs) have a broad size distribution from 20 to 350 nm but CNPs have a small and narrow particle size distribution from 2 to 6 nm (Figure 2a,b). Both CPs and CNPs have well graphitization, the interlayer spacing between graphitic sheets is $d_{(002)} = 0.33$ nm (obtained from HRTEM, shown as the inset in Figure 2b), which is very close to that of the ideal graphite. A similar type of carbon nanoparticle (1.5−2.5 nm) is reported earlier, following an aqueous route with the help of a silica sphere as carrier.[13] Comparison of TEM and fluorescence data shows that CNPs with a size of 2−6 nm have higher fluorescence intensity compared with CPs with a larger overall size. This type of size-dependent fluorescence QY is observed for carbon particles produced via laser ablation technique,[4] thermal decomposition,[11,13] and particles obtained from candle soot.[8]

We found that our CPs and CNPs have a very strong tendency of aggregation during TEM grid preparation or SEM slide preparation. The aggregation is so high that we face difficulty in finding significant amounts of isolated small carbon particles (CNPs) under TEM either from as-synthesized carbon particle (CP) solution or from CNP solution. A similar type of aggregation is observed by Iijima et al.,[20] where small carbon particles are found to aggregate into ∼80 nm size nanohorn structures. We have done some control SEM experiments to study this aggregation processes. Particle solution has been deposited on a Si substrate by a single or successive multiple drops (after the evaporation of the first drop, the next drop was added). We have always found that the multiple drop sample shows larger particles than the single drop. We have estimated the particle size of CNPs as 12−15 nm for the single drop sample (Figure 2c), but size increases when the sample was prepared from three drops (Figure 2d). This observation further indicates that the CNPs agglomerate easily in solid form but remain isolated in water. The AFM study of CNPs also showed the existence of small particles as well as particle aggregates even if a very dilute solution was used for this study (Figure S2, Supporting Information). We have also estimated the particle sizes of CPs and CNPs from the dynamic light scattering (DLS) measurement, and the result shows that the hydrodynamic diameters are broad and ranges from 20 to 350 nm for CPs; for CNPs, it shows a narrow distribution with an average diameter of ∼12.5 nm (Figure S3, Supporting Information). The broad size distribution and larger sizes in CPs mask the presence of small carbon particles (CNPs) in their size distribution. This broad DLS size distribution of CPs and narrow size distribution of CNPs corroborate the TEM observation. The increased average size of CNPs in the DLS study (in comparison with TEM, which shows 2−6 nm) is because DLS considers the overall hydrodynamic diameter that includes particles as well as adsorbed molecules and ions.

The soot contains mainly elemental carbon and oxygen, having 96 and 4 atom %, respectively, whereas the CNP shows that the C, O, and N are 59, 37, and 4 atom %, respectively, as

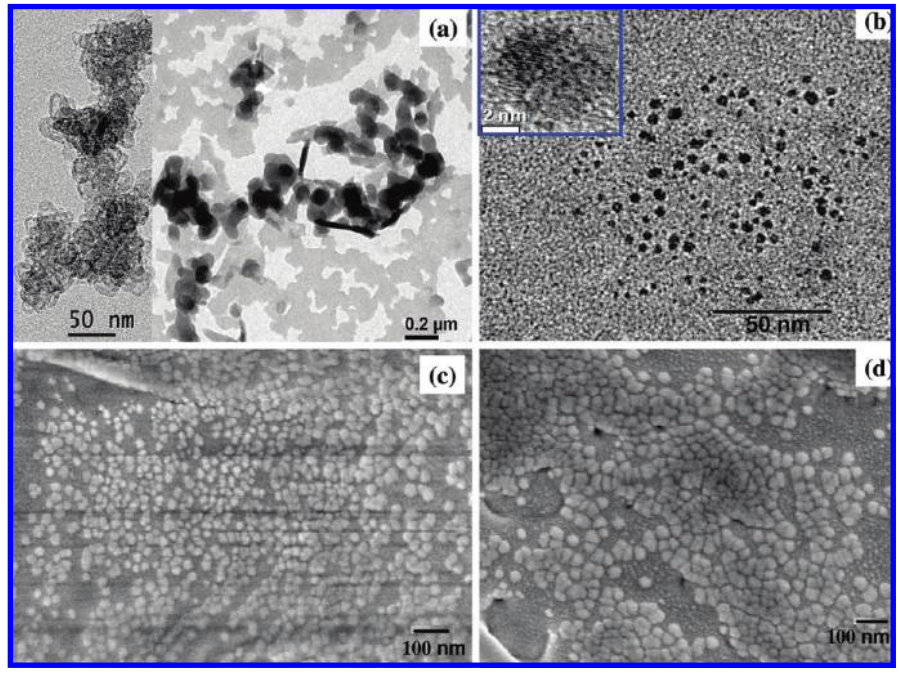


**Figure 2.** (a) Transmission electron microscopy (TEM) images of as-synthesized carbon particles (CPs), showing a broad size/shape distribution as well as extensive particle agglomeration. (b) TEM images of small sized carbon particles (CNPs) with a high-resolution image of one particle in the inset. (c) Scanning electron microscopy image of a single drop of CNP solution onto a Si substrate. (d) Scanning electron microscopy image of CNP solution on a Si substrate, but after having three successive drops. It shows that particle sizes increase due to agglomeration.



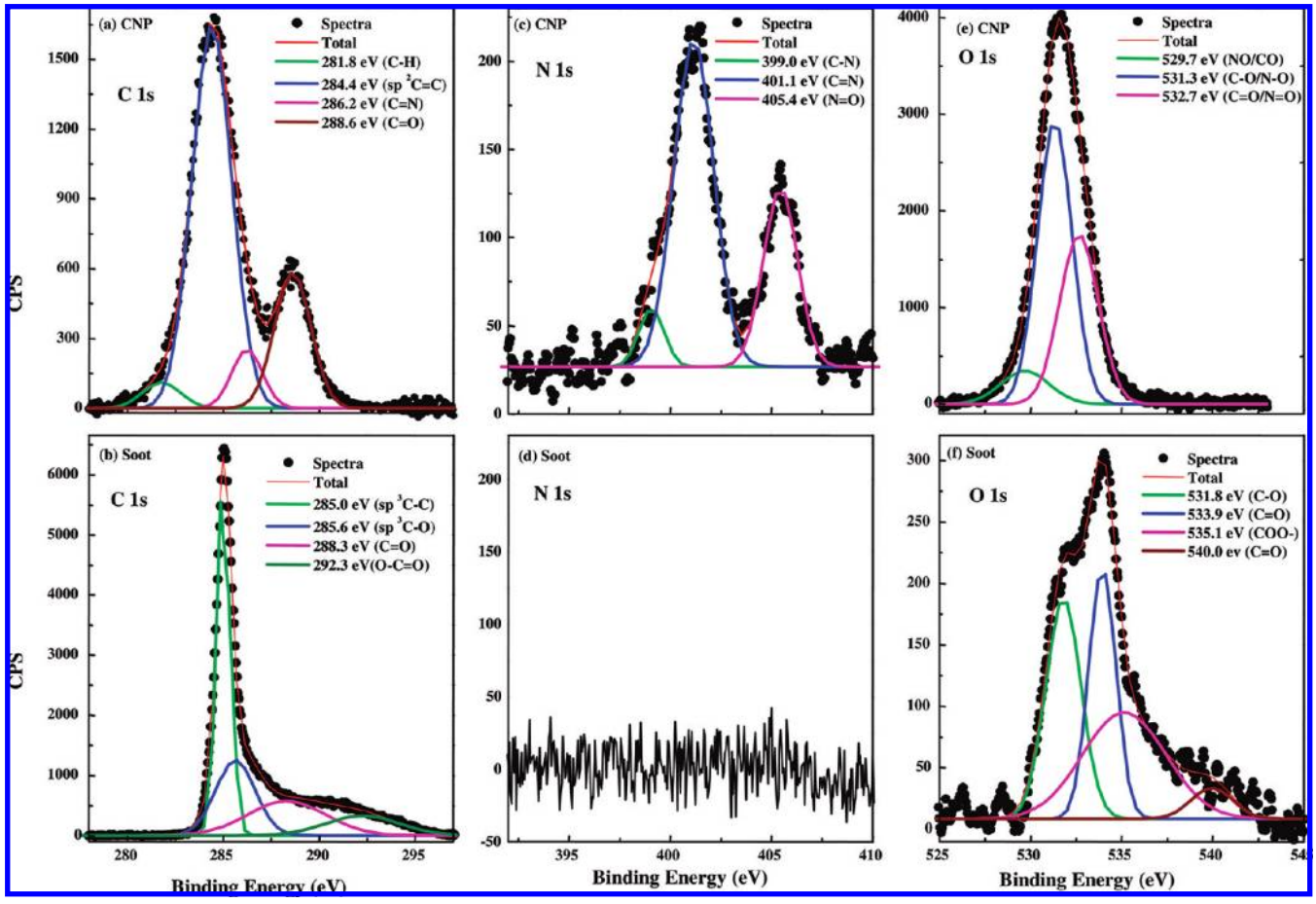


**Figure 3.** X-ray photoelectron spectroscopy (XPS) spectra of (a) C 1s, (c) N 1s, and (e) O 1s of CNP solution deposited on a glass substrate and (b) C 1s, (d) N 1s, and (f) O 1s of raw candle soot (powder). XPS compositional analysis shows a significant change in the percentage distribution of elements, from 96% C and 4% O in raw candle soot to 59% C, 37% O, and 4% N in the CNPs.

estimated from XPS compositional analysis. (Figure 3a−f). These data show that CNPs are mainly composed of graphitic carbon ($sp^2$) and oxygen/nitrogen-bonded carbon, whereas the starting soot is mainly composed of diamond-like carbon ($sp^3$)

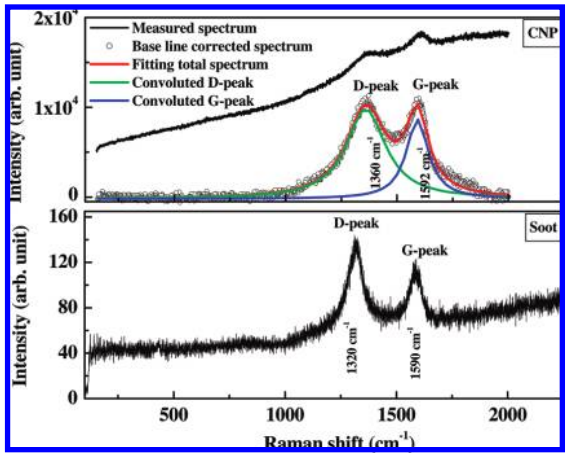


**Figure 4.** Raman spectra of CNPs and raw soot (powder). Fitting curve of the baseline corrected spectrum of CNPs shows the clear D and G peaks, and their intensity ratio, that is, ($I_D/I_G$), is equal to 2, which indicates that the structure of CNPs is nanocrystalline graphite.

with oxygen-bonded carbon.[21−33] This composition variation is well-matched with bonding structures obtained from the FTIR spectrum (see Figure S4, Supporting Information, and identification of different bonding configurations).[34,35]

Figure 4 shows the Raman spectra of the CNPs and soot. The spectrum of CNPs shows a high photoluminescence background compared with soot. The two signature peaks for carbon, that is, the D band and G band, are clearly seen for CNPs and soot, where the D band corresponds to the disordered structure in crystalline of the $sp^2$ cluster and the G band corresponds to the in-plane stretching vibration mode $E_{2g}$ of single-crystal graphite. The intensity ratio ($I_D/I_G$), which is often used to correlate the structural purity to the graphite, also indicates that the CNPs are composed of mainly nanocrystalline graphite.[35] The size of the nanocrystalline graphite obtained from the relation deduced by Ferrari et al.[35] was calculated as 2.2 nm. A similar graphitic structure is also obtained from X-ray diffraction patterns of CNPs (Figure S5, Supporting Information).

It is well-known that nitric acid oxidation produces OH and $CO_2H$ groups on the carbon nanoparticle surfaces, which made them hydrophilic and negatively charged particles.[36] In addition, this oxidation can also induce a small extent of nitration into graphitic carbon.[37] Our experimental data suggest that the refluxing step with nitric acid has made 2-fold chemical modifications to the soot. First, it induces partial oxidation of carbons and introduces functional groups, such as OH, $CO_2H$, and $NO_2$. Second, it induces doping of nitrogen and oxygen into the carbon particle. Introduction of functional groups induces water solubility and surface charge to the CNPs. In addition, it helps to break the large aggregated soot particle into small carbon particles. This oxidation step can also be considered as a chemical route of incorporating nitrogen and oxygen into the carbon particle, as observed from the chemical composition analysis.

The yield of soluble carbon particles depends on the oxidation property of nitric acid in refluxing condition, whereas the fluorescent quantum yield of carbon particles seems to depend on the efficiency of nitrogen and oxygen incorporation. Smaller particle size and dominant graphitic structure of the raw soot made this oxidation step easier. However, the efficiency of converting soot into soluble carbon particles is still low (yield ~20%), as observed from the large part of insoluble soot. This suggests that this type of chemical oxidation is not efficient enough for complete conversion into water-soluble particles. A longer time refluxing with nitric acid increases the yield of soluble particles to some extent but does not increase the yield of fluorescent carbon particles. This suggests that further oxidation might have other adverse effects, such as further oxidation of carbon particles that reduces the conjugated double bond structure in the carbon particle.

Incorporation of nitrogen and oxygen defects via nitric acid oxidation might have a role in producing a fluorescent center into carbon particles. Such defect structures in the fluorescence property of diamonds is well-established.[1,3] As soot has some percentage of diamond-like carbon (as observed from XPS data), it might happen that, during the oxidation step, nitrogen and oxygen defects are formed into the diamond structure. However, their presence in CNPs is too low to determine with our presented analytical method, and further study is needed to confirm this possibility. An alternative explanation of fluorescence may be that the chemical oxidation and doping steps introduce more conjugated double bond system into the carbon particle and thereby introduce the fluorescence property. Nevertheless, the advantage of this type of chemical processes of making fluorescent carbon particles is that it is simple and

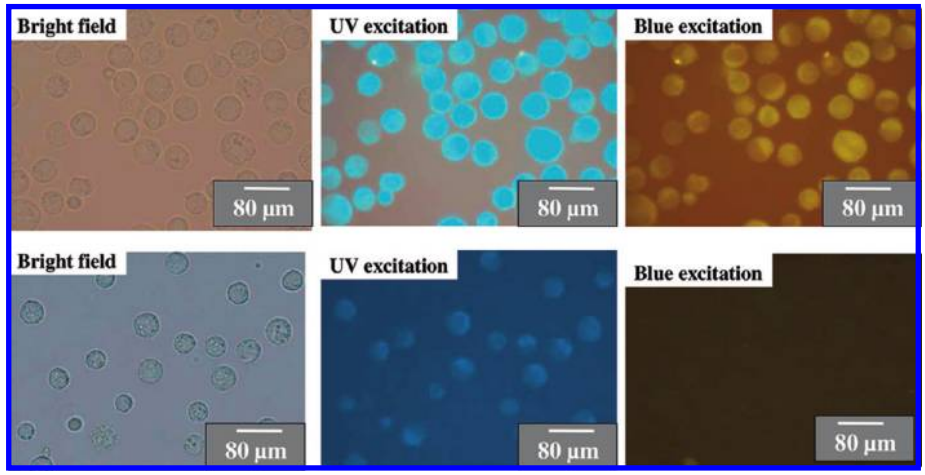


**Figure 5.** Fluorescent CNP-based labeling of EAC cells. The cell solution was mixed with CNP solution and incubated for 30 min. Washed cells were imaged under bright field, UV, and blue excitations. The bottom row images correspond to the control experiment where no CNP was used. Cells become bright blue-green under UV excitations and yellow under blue excitation, but they were colorless in the control sample. A light blue color of the control sample under UV excitation is due to the well-known autofluorescence of cells.

requires less adverse conditions as compared with the ion beam radiation method.[1,3] However, as-synthesized carbon particles have a heterogeneous size distribution, and small sized particles are more fluorescent than larger ones. Thus, successful isolation of small particles is essential for the enhancement of fluorescence quantum yield.

A water-soluble fluorescent carbon nanoparticle is an ideal cell-imaging probe with minimum cytotoxicity.[3,7,13] However, functionalization is an important step for cellular and subcellular targeting.[19] Interestingly, we found that small carbon particles (CNPs) enter into cells without any further functionalization, and using the fluorescence property of CNPs, it is possible track the CNPs (Figure 5). CNP solution has been mixed with cell culture media along with cells, incubated for 30 min, and washed cells were then imaged under bright field, UV, and blue excitations. Cells become bright blue-green under UV excitations and yellow under blue excitation, but they are colorless in the control sample where no CNP was used. This suggests that CNPs enter into the cells, and labeled cells can be imaged using a conventional fluorescence microscope. MTT and Trypan blue assays of cell viability studies suggest that CNPs have no cytotoxicity. We exposed the cells with CNPs of 0.1−1 mg/mL (which is about 100−1000 times higher than it required for imaging applications) for 24 h. The cell survival rate in <0.5 mg/mL was between 90% and 100%, suggesting a minimum cell death. However, at higher concentration, some percentage of cell death is observed. This result concludes that CNPs can be used in high concentration for imaging or other biomedical applications.

## Conclusion

Fluorescent carbon nanoparticles with a diameter of 2−6 nm were obtained after nitric acid oxidation of soot particles. Surface oxidation and subsequent nitrogen and oxygen doping afforded a light-emitting property of carbon particles. It is to be noted that the light emitted by these carbon particles depends on the wavelength of light used for excitation. We isolated different sized particles and found that the emission quantum yield is size-dependent, that is, the smaller the size, the better is their photoluminescence efficiency. Our approach can be used for milligram-scale synthesis of these water-soluble particles. The fluorescence property of these particles is useful for cell-imaging applications. These CNPs enter into cells without any further functionalization, and the fluorescence property of the particles can be used to track their position in cells using a conventional fluorescence microscope. The discovery of fluorescent carbon nanoparticles will no doubt lead to more research in this field; in particular, these particles have the potential in biomedical applications where cadmium-based quantum dots show toxic effects. However, synthetic methods of these particles need to be much more advanced so that large quantities of these particles with different emission colors can be easily prepared.

**Acknowledgment.** The authors would like to thank Dr. Nihar R. Jana of the National Brain Research Centre (NBRC), Gurgaon, India, for providing the cellular-imaging facility and cytotoxicity study. The authors would like to thank DST (SR/S5/NM-47/2005), Government of India, for providing financial support. A.S. thanks CSIR, India, for providing a fellowship.

**Supporting Information Available:** Fluorescence spectra of CPs produced at different reflux times and FTIR spectrum and AFM image of CNPs. This material is available free of charge via the Internet at http://pubs.acs.org.

## References and Notes

(1) (a) Gruber, A.; Dräbenstedt, A.; Tietz, C.; Fleury, L.; Wrachtrup, J.; von Borczyskowski, C. *Science* **1997**, *276*, 2012. (b) Neugart, F.; Zappe, A.; Jelezko, F.; Tietz, C.; Boudou, J. P.; Krueger, A.; Wrachtrup, J. *Nano Lett.* **2007**, *7*, 3588. (c) Batalov, A.; Jacques, V.; Kaiser, F.; Siyushev, P.; Neumann, P.; Rogers, L. J.; McMurtrie, R. L.; Manson, N. B.; Jelezko, F.; Wrachtrup, J. *Phys. Rev. Lett.* **2009**, *102*, 195506.

(2) (a) Glinka, Y. D.; Lin, K. W.; Chang, H. C.; Lin, S. H. *J. Phys. Chem. B* **1999**, *103*, 4251. (b) Zyubin, A. S.; Mebel, A. M.; Hayashi, M.; Chang, H. C.; Lin, S. H. J. *J. Phys. Chem. C* **2009**, *113*, 10432.

(3) Yu, S. J.; Kang, M. W.; Chang, H. C.; Chen, K. M.; Yu, Y. C. *J. Am. Chem. Soc.* **2005**, *127*, 17604.

(4) Sun, Y. P.; Zhou, B.; Lin, Y.; Wang, W.; Fernando, K. A. S.; Pathak, P.; Meziani, M. J.; Harruff, B. A.; Wang, X.; Wang, H.; Luo, P. G.; Yang, H.; Kose, M. E.; Chen, B.; Veca, L. M.; Xie, S. Y. *J. Am. Chem. Soc.* **2006**, *128*, 7756.

(5) Zhou, J.; Booker, C.; Li, R.; Zhou, X.; Sham, T. K.; Sun, X.; Ding, Z. *J. Am. Chem. Soc.* **2007**, *129*, 744.

(6) (a) Fu, C. C.; Lee, H. Y.; Chen, K.; Lim, T.; Wu, H. Y.; Lin, P. K.; Wei, P. K.; Tsao, P. H.; Chang, H. C.; Fann, W. *Proc. Natl. Acad. Sci. U.S.A.* **2007**, *104*, 727. (b) Wee, T.-L.; Tzeng, Y.-K.; Han, C.-C.; Chang, H.-C.; Fann, W.; Hsu, J.-H.; Chen, K.-M.; Yull, Y.-C. *J. Phys. Chem. A* **2007**, *111*, 9379. (c) Lim, T.-S.; Fu, C.-C.; Lee, K.-C.; Lee, H.-Y.; Chen, K.; Cheng, W.-F.; Pai, W. W.; Chang, H.-C.; Fann, W. *Phys. Chem. Chem. Phys.* **2009**, *11*, 1508.

(7) Gao, L.; Wang, X.; Meziani, M. J.; Lu, F.; Wang, H.; Luo, P. G.; Lin, Y.; Harruff, B. A.; Veca, L. M.; Murray, D.; Xie, S. Y.; Sun, Y. P. *J. Am. Chem. Soc.* **2007**, *129*, 11318.

(8) Liu, H.; Ye, T.; Mao, C. *Angew. Chem., Int. Ed.* **2007**, *46*, 6473.

(9) Zhao, Q.-L.; Zhang, Z.-L.; Huang, B.-H.; Peng, J.; Zhang, M.; Pang, D.-W. *Chem. Commun.* **2008**, 5116.

(10) Selvi, B. R.; Jagadeesan, D.; Suma, B. S.; Nagashankar, G.; Arif, M.; Balasubramanyam, K.; Eswaramoorthy, M.; Kundu, T. K. *Nano Lett.* **2008**, *8*, 3182.

(11) Bourlinos, A. B.; Stassinopoulos, A.; Anglos, D.; Zboril, R.; Georgakilas, V.; Giannelis, E. P. *Chem. Mater.* **2008**, *20*, 4539.

(12) Mochalin, V. N.; Gogotsi, Y. *J. Am. Chem. Soc.* **2009**, *131*, 4594.

(13) Liu, R.; Wu, D.; Liu, S.; Koynov, K.; Knoll, W.; Li, Q. *Angew. Chem., Int. Ed.* **2009**, *48*, 4598.

(14) Ushizawa, K.; Sato, Y.; Mitsumori, T.; Machinami, T.; Ueda, T.; Ando, T. *Chem. Phys. Lett.* **2002**, *351*, 105.

(15) Cahalan, M. D.; Parker, I.; Wei, S. H.; Miller, M. J. *Nat. Rev. Immunol.* **2002**, *2*, 872.

(16) Huang, L. C. L.; Chang, H. C. *Langmuir* **2004**, *20*, 5879.

(17) Kong, X. L.; Huang, L. C. L.; Hsu, C. M.; Chen, W. H.; Han, C. C.; Chang, H. C. *Anal. Chem.* **2005**, *77*, 259.

(18) Kong, X.; Huang, L. C. L.; Liau, S. C. V.; Han, C. C.; Chang, H. C. *Anal. Chem.* **2005**, *77*, 4273.

(19) (a) Medintz, I. L.; Uyeda, H. T.; Goldman, E. R.; Mattoussi, H. *Nat. Mater.* **2005**, *4*, 435. (b) Kamat, P. V. *J. Phys. Chem. C* **2008**, *112*, 18737.

(20) Iijima, S.; Yudasaka, M.; Yamada, R.; Bandow, S.; Suenaga, K.; Kokai, F.; Takahashi, K. *Chem. Phys. Lett.* **1999**, *309*, 65.

(21) Xia, Y.; Mokaya, R. *Adv. Mater.* **2004**, *16*, 1553.

(22) Baker, M. A.; Hammer, P. *Surf. Interface Anal.* **1997**, *25*, 629.

(23) Zheng, W. T.; Sjostrom, H.; Ivanov, I.; Xing, K. Z.; Broitmen, E.; Salaneck, W. R.; Greene, J. E.; Sundgren, J. E. *J. Vac. Sci. Technol., A* **1996**, *14*, 2696.

(24) Mansour, A.; Ugolini, D. *Phys. Rev. B* **1993**, *47*, 10201.

(25) Robinson, J. W. *Handbook of Spectroscopy*; CRC Press: Cleveland, OH, 1974; Vol. I.

(26) Paulmier, T.; Bell, J. M.; Fredericks, P. M. *Thin Solid Films* **2007**, *515*, 2926.

(27) Klages, K. U.; Wiltner, A.; Luthin, J.; Linsmeier, C. *J. Nucl. Mater.* **2003**, *56*, 313.

(28) Lukaszewicz, J. P. *J. Mater. Sci.* **1997**, *32*, 6063.

(29) Sato, T.; Narazaki, A.; Kawaguchi, Y.; Niino, H. *Appl. Phys. A: Mater. Sci. Process.* **2004**, *79*, 1477.

(30) Choi, H. C.; Park, J.; Kim, B. *J. Phys. Chem. B* **2005**, *109*, 4333.

(31) Yudasaka, M.; Kikuchi, R.; Matsui, T.; Kamo, H.; Ohki, Y.; Ota, E.; Yoshimura, S. *Appl. Phys. Lett.* **1994**, *64*, 842.

(32) Ghosh, P.; Zamri, M.; Subramanian, M.; Soga, T.; Jimbo, T.; Katoh, R.; Tanemura, M. *J. Phys. D: Appl. Phys.* **2008**, *41*, 155405.

(33) Wei, J.; Hing, P.; Mo, Z. Q. *Surf. Interface Anal.* **1999**, *28*, 208.

(34) Mutsukura, N.; Akita, K. *Thin Solid Films* **1999**, *349*, 115.

(35) Ferrari, A. C.; Robertson, J. *Phys. Rev. B* **2000**, *61*, 14095.

(36) Boehm, H. P. *Carbon* **1994**, *32*, 759.

(37) (a) Salame, I. I.; Bandosz, T. J. *J. Colloid Interface Sci.* **2001**, *240*, 252. (b) Kamegawa, K.; Nishikubo, K.; Kodama, M.; Adachi, Y.; Yoshida, H. *Carbon* **2002**, *40*, 1447.

JP905912N